

Article

## Comparing Whole Building Energy Implications of Sidelighting Systems with Alternate Manual Blind Control Algorithms

Christopher Dyke <sup>1,\*</sup>, Kevin Van Den Wymelenberg <sup>2</sup>, Ery Djunaedy <sup>2</sup> and Judi Steciak <sup>1</sup>

<sup>1</sup> Department of Mechanical Engineering, University of Idaho, Boise, ID 83713, USA; E-Mail: [jsteciak@uidaho.edu](mailto:jsteciak@uidaho.edu)

<sup>2</sup> Department of Architecture, University of Idaho, Boise, ID 83702, USA; E-Mails: [kevinv@uidaho.edu](mailto:kevinv@uidaho.edu) (K.V.D.W.); [erydjunaedy@gmail.com](mailto:erydjunaedy@gmail.com) (E.D.)

\* Author to whom correspondence should be addressed; E-Mail: [chrisdyke12@gmail.com](mailto:chrisdyke12@gmail.com); Tel.: +1-208-371-7871.

Academic Editor: Richard Mistrick

Received: 29 January 2015 / Accepted: 5 May 2015 / Published: 14 May 2015

---

**Abstract:** Currently, there is no manual blind control guideline used consistently throughout the energy modeling community. This paper identifies and compares five manual blind control algorithms with unique control patterns and reports blind occlusion, rate of change data, and annual building energy consumption. The blind control schemes detailed here represent five reasonable candidates for use in lighting and energy simulation based on difference driving factors. This study was performed on a medium-sized office building using EnergyPlus with the internal daylight harvesting engine. Results show that applying manual blind control algorithms affects the total annual consumption of the building by as much as 12.5% and 11.5% for interior and exterior blinds respectively, compared to the Always Retracted blinds algorithm. Peak demand was also compared showing blind algorithms affected zone load sizing by as much as 9.8%. The alternate algorithms were tested for their impact on American Society of Heating, Refrigeration and Air-Conditioning Engineers (ASHRAE) Guideline 14 calibration metrics and all models were found to differ from the original calibrated baseline by more than the recommended  $\pm 15\%$  for coefficient of variance of the mean square error (CVRMSE) and  $\pm 5\%$  for normalized mean bias error (NMBE). The paper recommends that energy modelers use one

or more manual blind control algorithms during design stages when making decisions about energy efficiency and other design alternatives.

**Keywords:** energy modeling; simulation; building performance; blind control; EnergyPlus

---

## 1. Introduction

It has been well documented that blinds affect energy use in buildings [1–4]; however, the application of blind control algorithms is not common in energy modeling practice. Buildings that use daylighting as a primary light source and rely on electric lighting only as needed have been shown to reduce annual lighting energy by up to 60% [1,3,4]. However, by controlling the amount of daylight and incoming solar radiation through the window, blinds affect interior lighting loads and space heating and cooling loads. There is an important trade-off between available daylight allowance and solar heat gain, and blind use impacts the relationship. In advanced motorized and automated blind systems, energy factors can be balanced to the greatest effect. However, most buildings rely on manual blinds and these are controlled by occupants following several influential factors including modulating the amount of daylight, minimizing glare, or for reasons of privacy or other factors [5].

Not only can blinds reduce cooling consumption, they can also reduce peak cooling demand. By controlling the incoming solar heat gains, the indoor temperature swings can be minimized, resulting in energy savings. Reducing peak cooling demand results in a smaller cooling system size, reducing capital costs. The use of blinds can be affected by several human factors as well as indoor and outdoor conditions. Correia da Silva *et al.* [2] describe how blind control patterns can be affected by illuminance and luminance, glare, solar radiation, and occupation period. Van Den Wymelenberg [5] categorizes several physiological and psychological reasons for manual blind operation. Each person has their own particular sensitivity to these triggers such as glare, view preference, and need for privacy; however, the literature suggests that the main reason behind blind control is direct solar radiation [5].

### 1.1. Window Shading Devices

Shading devices can be split into three types: internal, between-the-glass, and external. In this paper, “shades” or “blinds” may refer to any type of device (louver blinds, roller shades, overhangs, *etc.*) intended to control solar heat gain, glare or excessive sunlight penetration. Specifically, roller-shades or sheer shades are made of a cloth-like material (may be opaque, translucent or perforated) that can be retracted or engaged in part or fully, and “blind” suggests inclusion of angled louvers, and blinds therefore often provide more control options (engaged or retracted and louver tilt position).

Zhang *et al.* [6] cite results from a self-shading building where it was found that internal shading devices are more beneficial to east and west facades than to south facing facades. This suggests that orientation with respect to sun position has a significant impact on building performance. A literature review found a comparison of several case studies on blind occlusion (percent of blinds closed), blind rate of change, number of blind movements, and reasons for blind movement. One of the case studies

found that the South façade was the most triggered façade, and the north façade was the least triggered [5].

External shading devices are also an effective way to reduce incoming daylight and solar radiation. Not surprisingly, in most cases the most effective way to reduce solar heat gains on windows is to intercept direct solar radiation before it reaches the glass [7]. It was also noted that all external shading devices require free air movement to remove the heat that they absorb [7]. Between-the-glass shading devices include shades, blinds and adjustable glazing materials. It is important to note that by far the most common shading devices are manually operated interior louver blinds [8,9].

### 1.2. Shading Devices Control

Blind control falls into two categories: manual and automatic. Manual control of blinds relies upon occupants who typically make comfort- or preference-based decisions that can positively or negatively affect a building's thermal or visual performance. Occupants may close shading devices for many reasons and may not reopen them for a long time, perhaps weeks or months [2,5]. The literature suggests that the most commonly used scheme in evaluating energy demand is to assume shading devices remain in a fixed position during the entire year [2].

The second category of blind control is with automated systems, which can include interior or exterior components. The purpose of automated systems is to eliminate direct sun penetration because of glare potential or unwanted heat gain. Automatic systems can also include parameters to close blinds at night for privacy. The interaction between energy savings and building occupant desired control can prove to work against each other in certain situations.

A simulated automatic controls study performed by Congradac *et al.* [10] used a genetic algorithm based on fuzzy logic to control blinds and to save energy while maintaining thermal comfort within the design space. Simulation results found savings of 25% in the heating season and at least 35% in the cooling season by optimizing the blind tilt angle of interior louver blinds. The greatest savings were found on the South and West facades. By removing the need for occupants to manually operate shading devices, it can create a more comfortable environment as well as provide a system for incorporating the savings that would have been lost if blind position were left up to erroneous manual interaction. A case study performed on the New York Times Headquarters building suggest that automated blind control systems accounted for 98% of all blind movements [11]. The other 2% were results of user adjustment once a control decision is made by the automated system. Seventy percent of the human adjustments were to engage the blinds, suggesting the system was not as strict as desired by occupants.

### 1.3. Shading Device Control Triggers

For automated shading device control systems to work properly they must engage and retract shading devices based on certain triggers, or control indicators. These indicators help provide a controller with a range of allowable values that result in movement of shading devices. Reinhart [4] uses 50 W/m<sup>2</sup> of direct solar irradiance on the work plane as the threshold point before blinds are engaged. There are several different studies suggesting disparate control values of solar irradiance (11–325 W/m<sup>2</sup>) regarding the control trigger for blind engagement, and several metrics have been explored as blind

occlusion triggers [5]. Exterior vertical illuminance values of 41,000 and 50,000 lux showed the most agreement across studies as the trigger for engaging blinds, and values of 13,000 and 25,000 lux were found to be the most common trigger for retracting blinds. The difference between the trigger for closing and opening blinds is known as hysteresis. From a robust literature review, two manual blind control algorithms were proposed [5] and are explored here as proposed updates to the blind control algorithm Lightswitch-2002 [4]. The first algorithm, Blindswitch-2012A (henceforth referred to as Blindswitch A), occludes more windows as solar penetration depth increases once exterior irradiance normal to the sun exceeds  $120 \text{ W/m}^2$ . The second algorithm, Blindswitch-2012B (henceforth referred to as Blindswitch B), increase blind engagement as vertical exterior illuminance increases. Both proposed algorithms will be detailed in the methods section. Similar to Lightswitch-2002, Blindswitch-2012A and Blindswitch-2012B are date stamped so that they can be updated as more human factors research on blind use becomes available.

Correia da Silva *et al.* [2] cited several sources that have their own criteria for blind movement. Several available blind control algorithms were tested suggesting the algorithm that most closely represents the average resulting performance of all the algorithms tested should be used in future research. Their recommended trigger was using Daylight Glare Index (DGI) exceeding a value of 20 ( $\text{DGI}_{20}$ ) at a view angle of  $20^\circ$  towards the window. DGI is a measure of glare and is view and position factor dependent [12]. The  $\text{DGI}_{20}$  control strategy was one of several described by Correia Da Silva, but was deemed to most closely represent the average of all strategies studied [2].

#### 1.4. Purpose

There has been very little research up to this point on annual and subsequent energy end use distribution of manual blind control algorithms on existing buildings [5]. This paper hypothesizes that controlling blinds would have meaningful impact to whole-building energy and peak demand results in simulation. This paper identifies and compares five manual blind control algorithms (Blindswitch-2012A, Blindswitch-2012B,  $\text{DGI}_{20}$ , Always Engaged and Always Retracted) and reports detailed blind occlusion and rate of change data and subsequent annual building energy consumption. The purpose of the study is to determine how different the competing manual blind control algorithms are, and how impactful these differences may be to the practice of design analysis simulation.

These five algorithms were chosen based off of a literature review [2,5] which documented  $\text{DGI}_{20}$ , Always Engaged and Always Retracted as the most common blind triggers used in simulation. From a synthesis of real user data, the two additional candidate manual blind control algorithms were proposed (Blindswitch A and B) [5]. This paper establishes the need for changes to annual daylighting and energy simulation best practices.

A typical modeling assumption is to use blinds always engaged or always retracted in both daylighting and energy simulated building performance. This assumption can cause miscalculations in total building energy consumption and energy end use distribution (cooling, lighting, heating, *etc.*) [1,5]. Using annual simulated data derived without consideration of annual blind use patterns during design stages of a building can lead to poor design choices.

## 2. Methods

### 2.1. Case Study

The example building, built in 1999, is a three-story medium sized office building located in downtown Boise, ID, USA (Figure 1). Standard double pane ribbon windows, with a head height of 2.3 m measuring 1.5 m tall, span the entire perimeter of each floor. Open and private offices surround the perimeter of the building. The building is approximately 2973 m<sup>2</sup> in size and is dominated by core zones. The calculated building operational energy use intensity is 200 kWh/m<sup>2</sup>·year found from calibration of the existing building. Calibration of the energy model, per American Society of Heating, Refrigeration and Air-Conditioning Engineers (ASHRAE) Guideline 14–2002 [13], did not consider manual blind controls. This is typical of current building energy modeling best practices. Manual blind control is added to the original calibrated baseline model for this study. Daylight sensing electric lighting controls is applied and considers the location of blinds for each timestep investigated.



**Figure 1.** Case study building.

Windows have a  $U$ -value of 2.67 W/m<sup>2</sup>·K, solar heat gain coefficient (SHGC) of 0.497 and visual light transmittance (VLT) of 0.505 are used. A window-to-wall ratio of 35.7% is consistent across all three floors. Exterior walls and roof have a  $U$ -value of 0.036 and 0.19 W/m<sup>2</sup>·K, respectively. The building utilizes a built up heating, ventilation, and air conditioning system with water-to-air heat pumps at each zone. An 89% efficient boiler is used to provide heat to the water loop, and a two-speed cooling tower is used to reject the heat.

The actual building is oriented 32.4° counter clockwise from the North axis. For the purposes of this paper, the building's orientation was rotated (after calibration) so that facades matched true cardinal directions. Using these orientations allows for improved generalization of blind occlusion results based on specific façade orientation. Rotating the building showed a decrease in annual energy consumption of 0.8%–1.3% for the five blind control algorithms compared in this study.

The building was modeled using EnergyPlus version 7.0, a whole building energy simulation modeling program. By performing complicated thermal analyses the program serves to model the performance of buildings and optimize overall building design (Figure 2). Boise, ID typical meteorological year 3 (TMY3) dataset was used to represent typical rather than extreme weather conditions of actual yearly data.

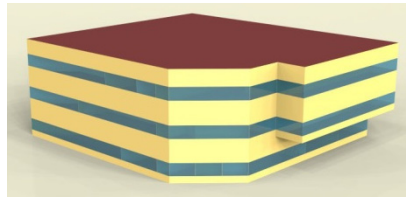


**Figure 2.** Case study energy model.

## 2.2. Daylight Harvesting

The daylight harvesting method used in this study incorporates a single analysis point per daylight zone [14]. Seven analysis points were used per floor totaling 21 illuminance sensor locations. Analysis point locations, centered on each of the three floors in perimeter zones, were a maximum depth of 3.05 m from the window. The EnergyPlus detailed daylight harvesting method was employed to obtain internal daylight illuminance values. This method also calculates the electric lighting load reduction caused by using available daylight.

## 2.3. Blind Control Algorithms for Simulation

Five blind control algorithms were considered to compare their relative differences. Table 1 lists the five manual control algorithms that were used in this study. Internal louver blinds were chosen as the primary shading device to compare control algorithms due to their prevalence in the built environment. External blinds were included in the annual consumption comparison to illustrate the dramatic effect of external *versus* internal blinds. While it is possible for external blinds to be operated via motors with manual control, buildings that invest in external blinds typically employ automated control sequences.

**Table 1.** Blind control algorithms.

Control Algorithm	Description
Always Engaged	Window blinds are always engaged
Always Retracted	Window blinds are always retracted
Blindswitch A	Window blinds engage with increased sun penetration depth and exterior irradiance > 120 W/m <sup>2</sup>
Blindswitch B	Window blinds engage following increased vertical exterior illuminance on façade
DGI <sub>20</sub>	Window blinds engage if Daylight Glare Index is above 20

## 2.4. Control Schemes

### 2.4.1. Always Engaged and Always Retracted

Occupants always leaving blinds either engaged (closed) or retracted (open) represent the extreme ends of the blind control spectrum. Previous research [3,15] identifies these static control schemes as important comparisons of conventional blind operation. The EnergyPlus *WindowProperty:ShadingControl* object is used with each window (*i.e.*, the *FenestrationSurface:Detailed* object). The *AlwaysOff* and *AlwaysOn* shading control types are used to simulate window blinds as always retracted (open) and engaged (closed), respectively. These algorithms do not demonstrate operable window blinds (meaning the blind can fully engage or fully retract); rather they are static blind position scenarios. The Always

Retracted algorithm is considered a second baseline model because it represents the same blind pattern (always open) but includes daylight sensing electric lighting controls (best case lighting savings). Always Retracted results will be compared to those of the baseline (no blinds, no daylight sensing lighting controls) and the Always Engaged models. By comparing Always Retracted results to the Always Engaged algorithm, both having daylight sensing electric lighting controls, it will demonstrate the energy implications strictly related to static engaged blind patterns.

#### 2.4.2. Blindswitch-2012A

The Blindswitch-2012A manual blind control algorithm is based on a trigger value of  $120 \text{ W/m}^2$  of exterior irradiance measured normal to the sun with increasing sun penetration depth resulting in more blinds engaged [5]. Once this trigger value is met, sun penetration depth and the amount of blinds engaged share a directly proportional relationship for a portion of the windows. The algorithm assumes that 5% of all blinds are always engaged and rotated closed (at a slat angle of  $75^\circ$  below the horizontal facing the window), 15% are always engaged but rotated open (at a slat angle of  $0^\circ$ , or horizontal), and 20% are always retracted. The remaining 60% of all blinds are considered operable (when engaged they have a slat angle of  $75^\circ$  below the horizontal facing the window). These blinds begin to retract when the exterior irradiance falls below  $120 \text{ W/m}^2$  or sun penetration depth falls below a setpoint for certain time duration. As seen in Figure 3, peak occlusion occurs at  $120 \text{ W/m}^2$  and a sun penetration depth of three meters. As exterior irradiation falls below  $120 \text{ W/m}^2$  or sun penetration depth falls below 1 m for three hours, all operable blinds are retracted. The algorithm follows a bi-directional linear relationship meaning the amount of blinds engaged will vary with the depth of sun penetration as seen in Figure 3, noting that blind retraction also follows the time delay illustrated. Exterior irradiance was treated as the primary trigger followed by sun penetration depth.

To generate this control algorithm it is important to understand the geometry of the model. The actual building has ribbon windows along the entire perimeter of each floor. To accurately recreate this control scheme, the ribbon window on each façade and floor must be broken into 10 separate windows. The actual window height is still used. The length of each window is proportional to a corresponding occlusion percentage for the Blindswitch-2012A algorithm (*i.e.*, the 5% portion of blinds always engaged and closed is equal to 5% of the total length of windows on each floor and façade of the building). Each window in the model was defined with a blind condition from the algorithm (10% always retracted, 5% always engaged and rotated  $75^\circ$ , 15% always engaged and horizontal, and 60% operating per the solar irradiance and penetration algorithm) in randomized fashion, and applied to the model. Figure 4 shows the random configuration and layout of the West façade windows. Each façade was treated with randomization in this manner. One issue caused by the randomization is the possibility that a window blind that is always engaged, may randomly be placed directly in front of a daylight sensor. This would result in very little electric light dimming due to the minimal amount of daylight available through the engaged and closed blind. This occurrence is considered appropriate because it represents a plausible reality of an occupant leaving a blind engaged with respect to the daylight analysis point in a real building.

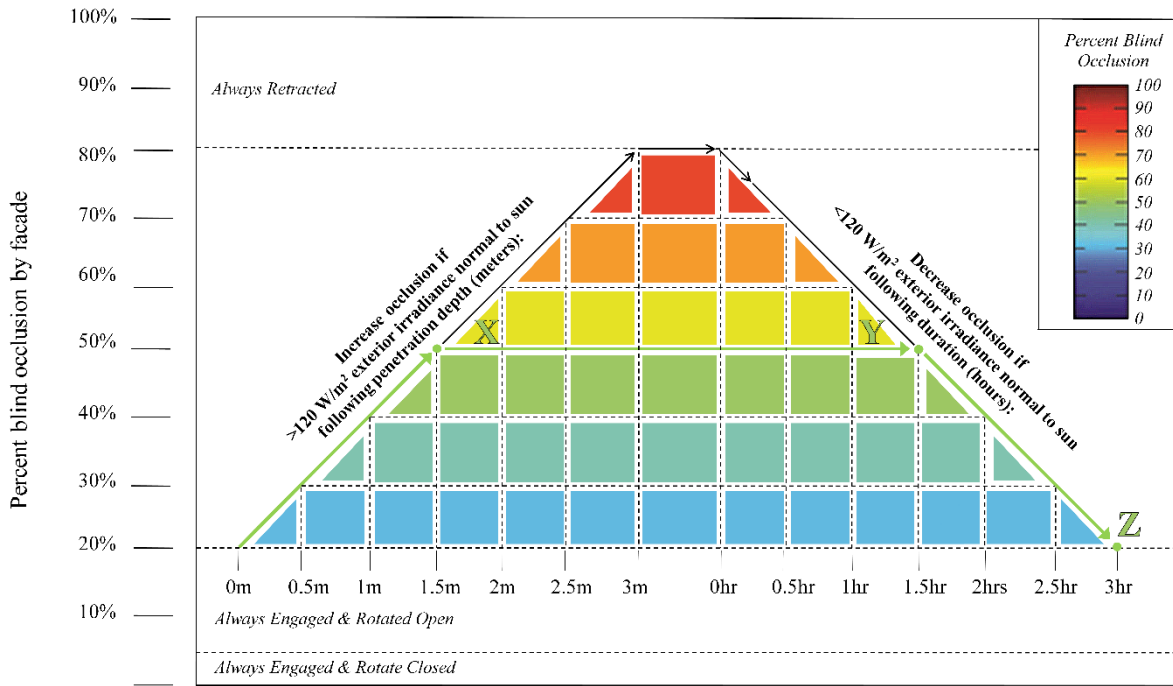


Figure 3. Operation algorithm for Blindswitch A—following Van Den Wymelenberg [5].

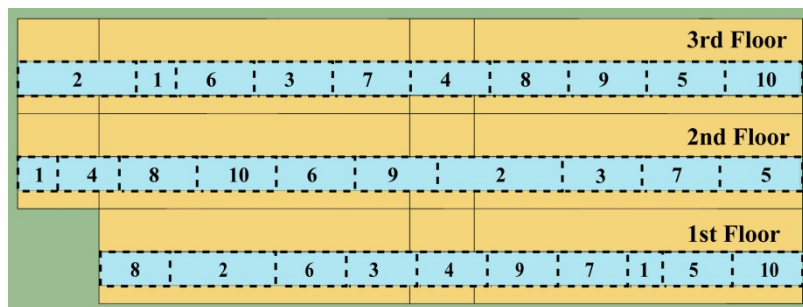


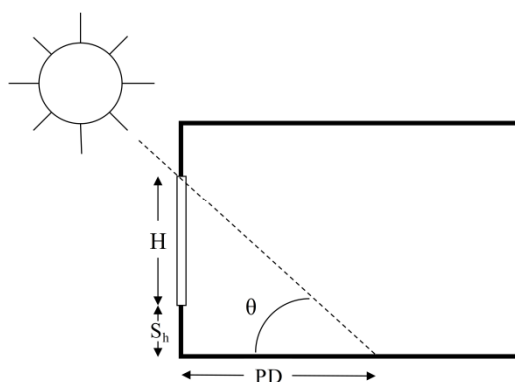
Figure 4. Window randomization of West façade.

Table 2 shows the control algorithm associated with each window orientation. By randomizing the initial window locations, a more realistic algorithm can be implemented based on the actual unreliability of blind occlusion. The term operable refers to the blind being adjustable within the control algorithm. The blind can either fully engage (blind completely covers window and slat angle is 75° below the horizontal) or fully retract (window is uncovered).

**Table 2.** Trigger values for manual blind control algorithm (Blindswitch A and B).

Window #	Control Scheme	Percent Occlusion	Blind Trigger Values			
			Blindswitch A		Blindswitch B	
			Engage blind after penetration depth in space $\geq$ value (m)	Retract blind after engagement triggers drop below for duration $\leq$ value (h)	Engage blind if vertical exterior illuminance $\geq$ value (lux)	Retract blind if vertical exterior illuminance $\leq$ value (lux)
1	Always Engaged & Rotated Closed	5%	–	–	–	–
2	Always Engaged & Rotated Open	15%	–	–	–	–
3	Operable	10%	0.5	3	33,000	17,500
4	Operable	10%	1	2.5	47,500	22,500
5	Operable	10%	1.5	2	60,000	30,000
6	Operable	10%	2	1.5	72,500	37,500
7	Operable	10%	2.5	1	86,000	42,500
8	Operable	10%	3	0.5	100,000	49,000
9	Always Retracted	10%	–	–	–	–
10	Always Retracted	10%	–	–	–	–

To model the control algorithm, the Energy Management System (EMS) within EnergyPlus was used. The EMS input allows a user to create custom algorithms that the basic control schemes of EnergyPlus are not capable of performing. The three trigger values for this algorithm include: exterior irradiance normal to the sun, sun penetration depth, and time duration. These trigger values were either extracted from the weather file or calculated two timesteps every hour. Because the weather file contains only hourly data, EnergyPlus calculates the weighted average for timesteps greater than one. In this case, EnergyPlus estimates the half hour value based on an average of the last hour and current hour values. Exterior irradiance values normal to the sun were gathered using the output *Direct Solar* from the weather file. Solar penetration depth was calculated using the *Solar Horizontal Profile Angle* output. The horizontal profile angle is defined as the angle between the window outward normal and the projection of the sun's ray on the vertical plane normal to the window. Because the angle is always normal to the surface the solar angle and azimuth angle are consistently taken into account.



**Figure 5.** Sun penetration depth.

Equation (1) was used to calculate sun penetration depth ( $PD$ ).  $H$  is window height (m),  $S_h$  is the sill height (m), and  $\theta$  is the horizontal profile angle. A sun penetration depth layout for a typical floor can be seen in Figure 5. The solar penetration depth calculation is the same for each floor because horizontal profile angle does not vary from floor to floor. A timestep of one half hour was used on Blindswitch-2012A to create a more accurate representation of the proposed hypothetical behavioral model [5]:

$$PD = \frac{(H + S_h)}{\tan \theta} \quad (1)$$

The Blindswitch-2012A algorithm decreases blind occlusion, the act of retracting blinds, as a function of a timed duration of exterior irradiance and solar penetration depth falling below specified intervals. To deal with this timed sequence trend variables were used within the EMS. Trend variables are useful because they allow the user to collect and analyze stored variables for a specified amount of timesteps. Trend variables are used extensively throughout the algorithm. To accurately achieve the control algorithm, each façade was broken into ten windows, each specified with a certain blind occlusion characteristic. Figure 3 shows the breakdown of trigger values of exterior irradiation, sun penetration depth, and time duration following the blind engaged and retracted lines. For example, the 40%–50% range of windows, simulated as one single window per façade and floor, will engage blinds after  $120 \text{ W/m}^2$  hits the façade (measured normal to the sun) and a sun penetration depth greater than

1.5 m is met (Point *X*). The blind will then retract after the exterior irradiation falls below  $120 \text{ W/m}^2$  for 1.5 h (Point *Y*) or sun penetration depths do not exceed 0.5 m into the space, and all operable blinds will retract after three hours below the trigger thresholds (Point *Z*). Similarly, each corresponding window group (dependent on percentage of blind occluded) will trigger blind engagement with increasing sun penetration depth, and will then retract with shorter elapsed time periods. The specific trigger points seen in Figure 3 for each window are displayed in Table 2.

### Control Algorithm

The control decision progression made for each operable window groups 3–7 at each timestep follows a stacked decision scheme, meaning conditional statements are built upon each other. The controller will jump to the next line if the previous statements returns false. The conditional programming is developed using the *EnergyManagementSystem:Program* object in EnergyPlus. When a line returns a true condition a blind status is sent to the *EnergyManagementSystem:Actuator* which controls the operability of the blind. Each decision in the program corresponds to a specific situation typically seen with respect to direct solar and sun penetration depth. The previous and maximum values seen in the decision scheme are calculated using trend variables in EMS. The maximum previous horizontal profile angle for the last number of timesteps (dependent on retraction trigger duration from Table 2) was used to calculate sun penetration depth. Because solar penetration depth can only be calculated during the current timestep, the horizontal profile angle variable was used to perform this function. The trigger values horizontal profile angle used to calculate sun penetration depth are shown in Table 3. The blind position of the next window is also considered in this scheme. Window operability order is pre-set (although location is randomized); blinds for window No. 3 engage first, while blinds for window No. 8 engage last. This allows the manual blind control algorithm to function based on other blind positions, representing a dependent system.

The same control algorithm is applied to each operable blinds 3–7. Blind 8, for each façade and floor, had a slightly different control scheme. Because it is the last operable blind on each façade and floor, it is only dependent on the exterior irradiation and solar penetration depth. A flow chart of the described processes can be found in available literature [14].

**Table 3.** Trigger values for manual blind control algorithm (Blindswitch A).

Window #	Sun Penetration Depth (m)	Horizontal Profile Angle (°)
3	0.5	77.9
4	1.0	66.8
5	1.5	57.3
6	2.0	49.4
7	2.5	43.1
8	3.0	37.9

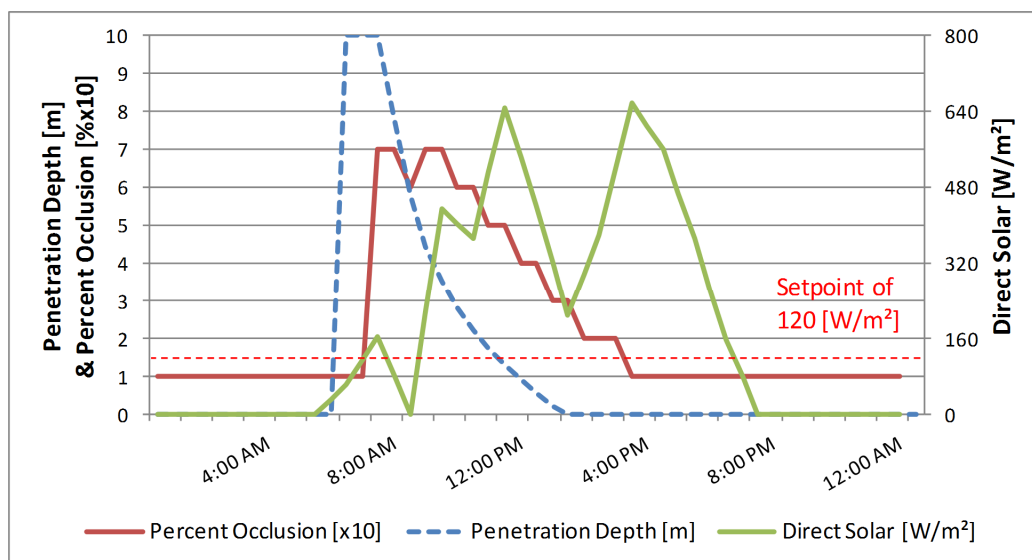
### Verifying Model Operation

Percent occlusion is based on a ratio of the number of blinds engaged compared to total number of blinds [16]. The orientation and use of blinds depending on time of year was the topic for this study.

An occlusion value was given to each window dependent upon blind height (0–5 point scale) and blind tilt (1–3 point scale). The points were then multiplied which result in an overall occlusion value. Percent blind occlusion for Blindswitch-2012A and Blindswitch-2012B can be seen in Equation (2). From this equation, the minimum percentage of blinds always engaged is 10%, and the most at any given time is 70%. The cumulative 30% always retracted is the result of the control algorithm detailed in Section 2.4.2 and Equation (2):

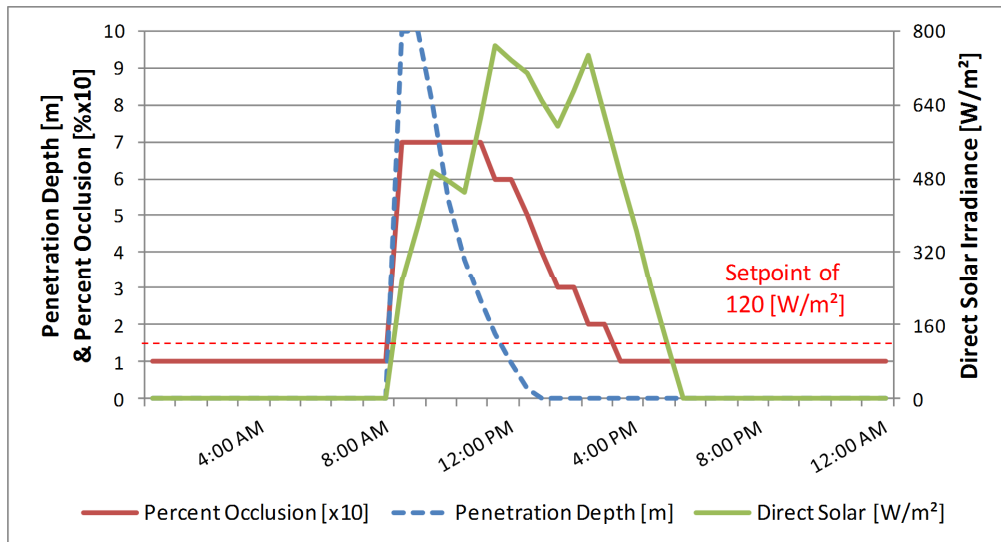
$$\% Occlusion = \frac{1}{20} * \frac{5}{5} * \frac{3}{3} + \frac{3}{20} * \frac{5}{5} * \frac{1}{3} + \frac{1}{10} * \frac{5}{5} * \frac{3}{3} * (\# \text{ of engaged blinds}) + \frac{1}{10} * \frac{0}{5} * \frac{1}{3} \quad (2)$$

Periods of time that provided substantial variety of direct solar radiation and sun penetration depth throughout the day were chosen to show the flexibility of the model. 22 April contains an event, as seen in Figure 6, where the direct solar exceeds 120 W/m<sup>2</sup> and sun penetration depth on the East façade first floor exceeds three meters, causing full occlusion of the blinds per Blindswitch-2012A (70%). Shortly after the initial engagement of blinds (8:30 a.m.), direct solar falls below 120 W/m<sup>2</sup> for a long enough duration to cause a small percentage of blinds to retract, seen by the blind retraction percentage. Direct solar then rises above 120 W/m<sup>2</sup> again to cause full occlusion (70%) on the façade. The control algorithm response is displayed as percent occlusion *versus* time. Sun penetration is shown to peak at 10 m on the East facade, when in reality the sun will penetrate much deeper into the space. Because no zone has a depth greater than 10 m, and once penetration depth reaches 3 m the façade will be at full occlusion for the operable blinds, solar penetration is shown to peak at 10 m even though in reality the calculated depth may be theoretically greater.



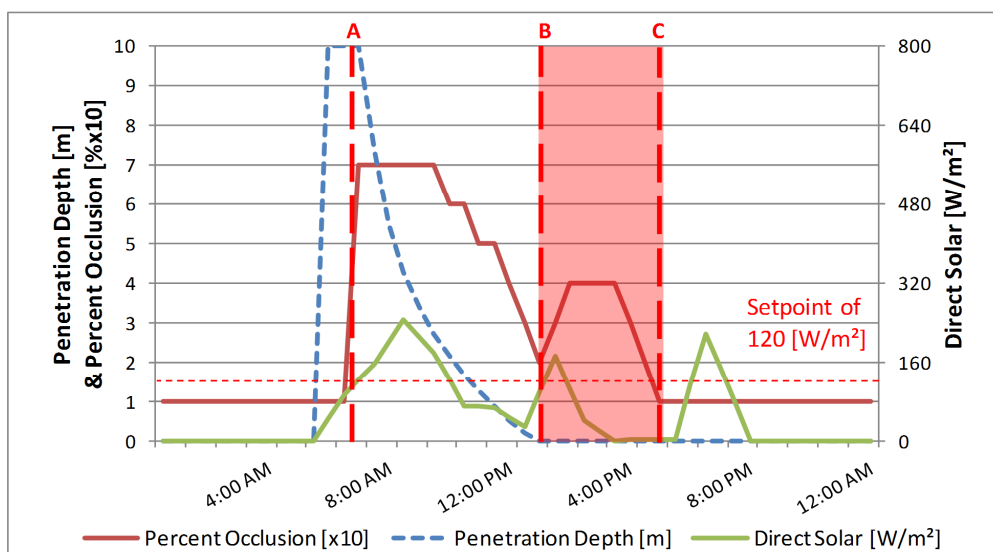
**Figure 6.** Hourly control algorithm response for east façade first floor on 22 April (Blindswitch A).

Figure 7 demonstrates a typical winter day, 5 December, on the East façade first floor with a large amount of direct solar radiation and sun penetration depth in the morning, decreasing as the day progresses. An important aspect of this time frame is that as sun penetration depth reduces, only 10% of the blinds can retract per timestep. This ensures the simple progression of blind retraction as solar radiation and sun penetration depth decrease.



**Figure 7.** Hourly algorithm response for east façade first floor on 5 December (Blindswitch A).

Verifying algorithm accuracy showed one particular problematic issue. The problem only occurs in Blindswitch-2012A, and is seen in Figure 8, when solar irradiance and sun penetration depth rise above their respective trigger values during the afternoon (Point A) and then fall below the trigger value for the maximum duration allowed before most operable windows are retracted (Point B). Once blinds retract, the direct solar quickly rises above the  $120 \text{ W/m}^2$  trigger value with no daylight penetration depth (Point C). From Point B to Point C corresponds to incorrect control responses. A line of code in the control algorithm causes the blinds to stay engaged even though the sun penetration depth is far below the required trigger value to cause occlusion. This line of code is imperative [14] because it ensures that each blind stays engaged for the required duration even though trigger values are unmet. This limitation is a result of the algorithm not the EnergyPlus EMS. It would be possible to fix the issue using the EnergyPlus EMS, but was considered not practical to complete in the scope of the study. The frequency of the error occurrence was calculated to ensure minimal error. By using strictly the direct solar irradiance from weather files, the errors were calculated and obtained.



**Figure 8.** Hourly typical error of blind control algorithm on 26 April (Blindswitch A).

Six weather files were tested with results seen in Table 4. The error occurs most often in Golden, CO, at 35 timesteps per year. This corresponds to 17.5 h per year, with an annual error rate of 0.39% of daylight hours. The errors found were determined to be the worst possible scenario. A maximum error rate of 0.39% was deemed to be acceptable.

**Table 4.** Blindswitch A errors.

Location	Timestep Error Occurs (1/2 h Each)	Total Hours	% of Daylight Hours Per Year
Boise, ID	14	7	0.16%
San Francisco, CA	4	2	0.04%
Chicago, ID	15	7.5	0.17%
Tampa, FL	11	5.5	0.12%
Golden, CO	35	17.5	<b>0.39%</b>
Tucson, AZ	7	3.5	0.08%

#### 2.4.3. Blindswitch-2012B

The second manual blind control algorithm, Blindswitch-2012B, is based on a proportional relationship between vertical exterior illuminance and percent occlusion, as seen in Figure 9 [5]. The operable window blinds engage when exterior illuminance rises above 33,000 lux. A main aspect of this algorithm is the hysteresis effect once the maximum illuminance value is met. Blinds will remain engaged until specific reduced illuminance values for retraction occur, as seen on the blind retraction line of Figure 9. The same horizontal hysteresis is seen for each window percentage. For example, as seen in Figure 10, if during the day the maximum exterior illuminance seen on a façade reaches 60,000 lux, then 50% of blind will engage (Point X). Once exterior illuminance falls below 30,000 lux (Point Y), blinds retract to the minimum 20% (Point Z). Dotted lines, in Figure 9, represent blind retraction triggers points.

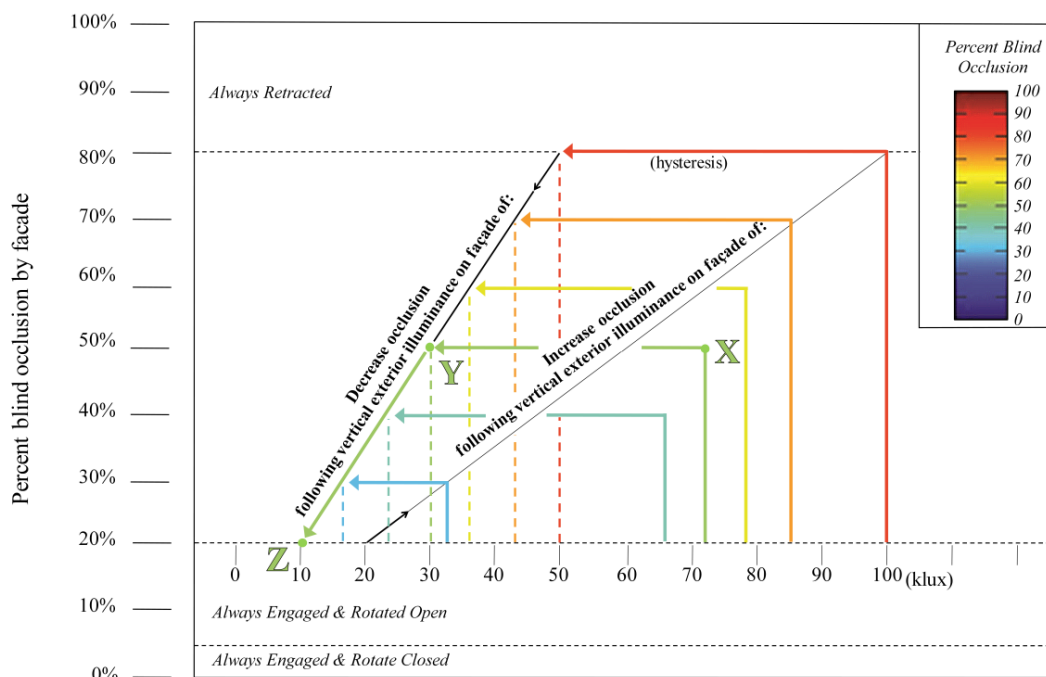


**Figure 9.** Operation algorithm Blindswitch B—following Van Den Wymelenberg [5].

## Algorithm Implementation

To recreate this control algorithm, the same application of 10 windows per façade and floor was used as in Blindswitch-2012A. The scheme shown above was broken up into 10 separate control points. Figure 9 demonstrates the control points broken up with a color map. Table 2, in Section 2.4.2, also lists the control points for each of the windows. To implement this control algorithm the model was run with one-hour timesteps and 10 window groups per façade and floor. The fixed blinds were treated the same as in Blindswitch-2012A, which means 5% of blinds were engaged but rotated closed, 15% of blinds were engaged but rotated open, 20% were always retracted, and 60% were operated according to the exterior illuminance algorithm.

## Control Algorithm

The EnergyPlus EMS was also used to create Blindswitch-2012B. Trend variables were used to track previous blind positions. Using the trigger values outlined in Table 2 the algorithm can be tailored to each window type. Vertical exterior illuminance was the main trigger of this manual blind control scheme. Values were obtained using the daylight analysis engine Radiance by placing one exterior analysis point per floor and façade at the work plane level (0.76 m) just outside the window. Typically, exterior illuminance rises, peaks at different times of the day depending on the façade orientation and sun position, and then drops. This limited variability simplifies the control algorithm compared to Blindswitch-2012A, as documented elsewhere [14].

### 2.4.4. Daylight Glare Index

A manual control algorithm based on Daylight Glare Index (DGI) is compared [2]. The control strategy  $DGI_{20}$  is based on the assumption that the occupants will engage internal blinds when DGI exceeds a value of 20, with a view direction of  $20^\circ$  towards the window (Figure 10). DGI is a calculation of daylight discomfort glare based on view direction. The view direction is adjusted in the model to represent a typical seating orientation, which is at a slight angle towards the window. The control algorithm then retracts the blinds when DGI falls below the threshold value of 20.  $DGI_{20}$  was chosen by Correia da Silva *et al.* [2] because it leads to the closest results with respect to the average of all the simulated strategies they tested.

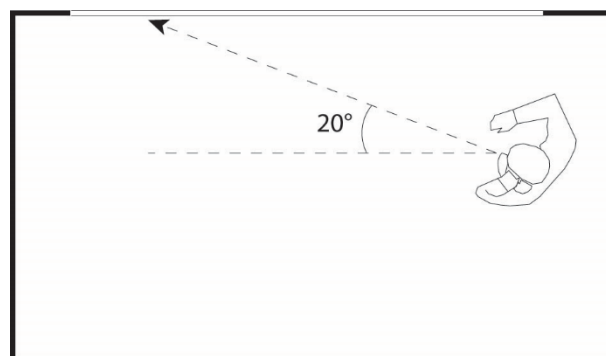


**Figure 10.** View angle ( $DGI_{20}$ ).

EnergyPlus contains a glare based controller in the *WindowProperty:ShadingControl* object that was used in conjunction with a daylight analysis point. Analysis point locations were centered on all three floors in perimeter zones at a maximum depth of 3.05 m from the window [14]. Seven sensors were used per floor, totaling 21 for the entire building. The Hopkins formula [17], Equation (3), was used to calculate daylight discomfort glare at each analysis point, *i.e.*, each sensor. The gross glare index ( $G_I$ ) is a function of the glare constant from each window viewed at each analysis point, seen in Equation (4):

$$G = \frac{L_w^{1.6} \cdot \Omega^{0.8}}{L_b + 0.07 \cdot \omega^{0.5} \cdot L_w} \quad (2)$$

$$G_I = 10 \cdot \log_{10} \sum_{i=1}^{\# \text{ of windows}} G \quad (3)$$

where  $G$  is the discomfort glare constant,  $L_w$  is the average luminance of the window as seen from the reference point ( $\text{cd}/\text{m}^2$ ),  $\omega$  is the solid angle subtended by the window with respect to the reference point,  $\Omega$  is the solid angle subtended by the window modified to take occupant view direction into account, and  $L_b$  is the average luminance of the background area surrounding the window. If the glare index at the reference point exceeds the set point then zonal windows are shaded one by one until the glare index falls below the set point. The *OnIfHighGlare* shading control type was used with a glare setpoint applied at each *Daylighting:Controls* object. A fixed slat angle of  $75^\circ$  below the horizontal facing the window was used for engaged blinds, which represents the actual building blind construction. The same randomized window group layout used with *Blindswitch-2012A* and *Blindswitch-2012B* was applied to the *DGI<sub>20</sub>* model. Figure 11 displays the view angle of each analysis point used in *DGI<sub>20</sub>*. The  $20^\circ$  angle used is the view clockwise of window orientation. For example, each West façade analysis point has a  $200^\circ$  rotation from the absolute north axis; therefore, the analysis point actually sees more of a south facing direction. The same relation view direction is seen for each respective façade.

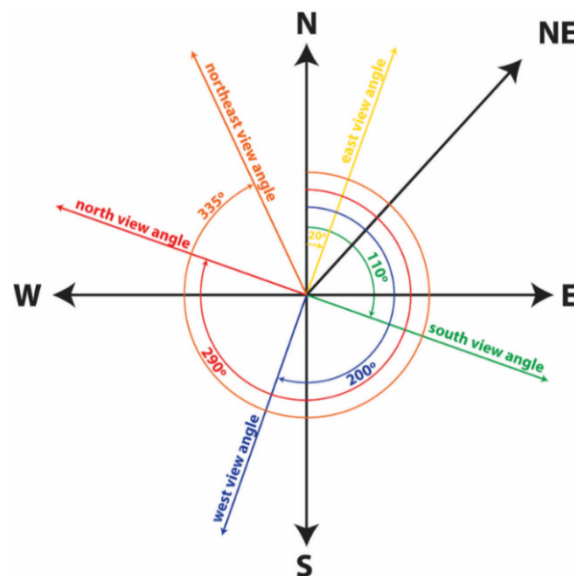


**Figure 11.** Analysis point view angles (*DGI<sub>20</sub>*).

### 3. Results

#### 3.1. Blind Rate of Change

One way to compare the pattern of blind use is to measure blind adjustment frequency, or “rate of change” [5,18,19]. DGI<sub>20</sub>, and Blindswitch A and B were compared to show relative differences in average daily rate of change averaged from all the three floors. Rate of change, ROC [5], calculated using Equation (5), is based solely on blind movement per façade: a particular blind either engages or retracts. ROC does not take into account the number of times the blind changes throughout the day. Therefore, the number of blind movements, NBM [5], was calculated using Equation (6). NBM is a ratio of the total number of blind movements per day to the total number of blinds that moved (at least once) per day per façade:

$$ROC = \frac{\sum_{n=1}^{\# \text{ of blinds per facade}} \begin{cases} 1 & \text{if blind moves at least once per day} \\ 0 & \text{if there is no blind movement} \end{cases}}{\text{Total \# of windows per facade}} \quad (4)$$

$$NBM = \frac{\sum_{n=1}^{\# \text{ of blinds per facade}} (\# \text{ of blind movements per day})}{\text{Total \# of blinds that moved per day}} \quad (5)$$

Table 5 summarizes the results found for ROC on three of the advanced blind control algorithms on an annual basis. DGI<sub>20</sub> results in the largest average rate of change and number of blind movements per day, followed by Blindswitch A. It is interesting to note that DGI<sub>20</sub> never results in zero ROC. Therefore, DGI<sub>20</sub> proves to be the most active blind control algorithm of all three. On the East and South façade, Blindswitch A reaches a maximum ROC value of 60% throughout the entire year. This is caused by the 40% of blinds considered non-operable, as detailed in Section 3.2.3. The South façade of the Blindswitch A and DGI<sub>20</sub> models results in the highest annual average of 34% and 93% ROC, respectively. The DGI<sub>20</sub> model results in highest annual average in the East at 57%. The North façade, not surprisingly, resulted in the lowest ROC values for all three algorithms.

**Table 5.** Annual average ROC and NBM [14].

Annual Average Rate of Change				
Model	East	South	North	West
Blindswitch A	48%	34%	23%	48%
Blindswitch B	23%	29%	0%	27%
DGI <sub>20</sub>	57%	93%	54%	60%
Annual Average Number of Blind Movements				
Model	East	South	North	West
Blindswitch A	1.89	1.99	1.43	1.66
Blindswitch B	1.51	1.82	0.00	1.60
DGI <sub>20</sub>	2.64	3.16	2.65	2.48

NBM values, also seen in Table 5, for the West, East and South facades averaged from all three floors for Blindswitch A and B show a consistent value of 2. This corresponds to a typical blind operation of engaging a blind once in the morning and retracting once in the afternoon/evening. Overall, other than the North façade, Blindswitch A and B showed similar results for ROC and NBM [14].

### 3.2. Average Percent Occlusion

#### 3.2.1. Blindswitch-2012A

Several factors were taken into account when comparing the results of the analysis for Blindswitch A. Percent occlusion per façade and floor, based on total annual hours (8760) were compared to show the effect that orientation has on blind operation in this algorithm. Annual average occlusion values for each façade and floor can be seen in Figure 12. The North façade resulted in the lowest amount of occlusion mainly because it typically sees the least amount of sunlight penetration throughout the year. The South facade resulted in the largest annual average percent occlusion (21.9%). Results show floor height does not affect percentage occlusion with Blindswitch A. Blindswitch A also shows that there is no consistent response per orientation of window, meaning each window orientation reacts differently to sun penetration and direct solar irradiance.

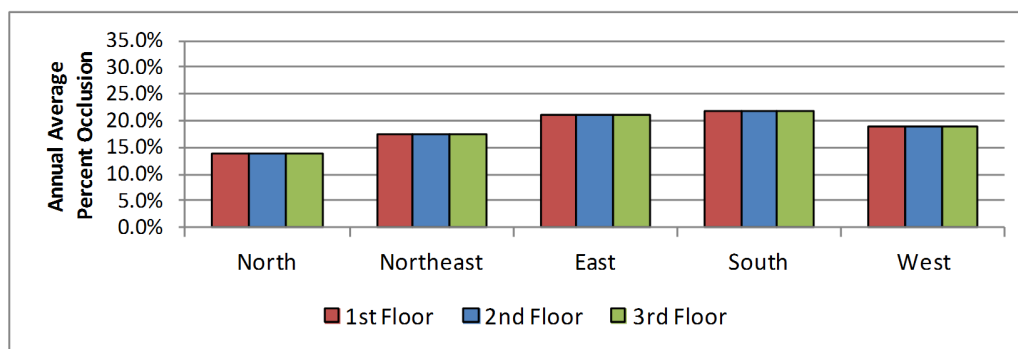


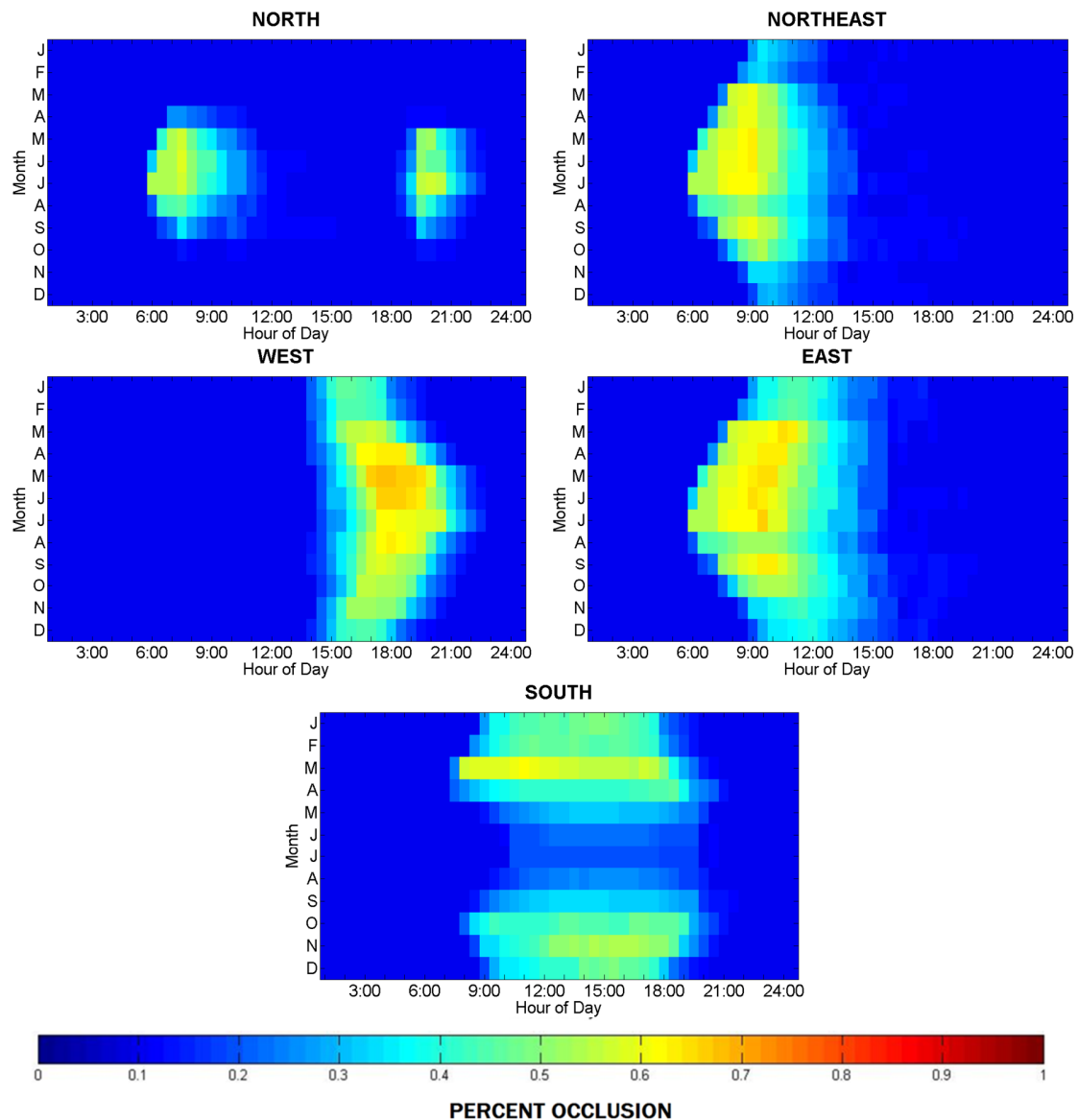
**Figure 12.** Annual average percent occlusion (Blindswitch A).

Color maps were used to compare occlusion percentage as a function of month of year and time of day. For each half hour of the day, occlusion percentages were averaged to show typical blind operation depending on the month of the year. Figure 13 shows these typical occlusion values for all five orientations on the second floor. The colors dark red and dark blue represent full blind engagement and retraction for the operable blinds, respectively.

In Figure 13, the typical occlusion percentages for every given hour and month of the year are included. The North façade follows a daily engagement/retraction scenario. Blinds begin engaging early in the morning (6 a.m.) during the summer months and retract around 12 p.m. Blinds then re-engage around 7 p.m. and completely retract around 9 p.m. Though typical office hours range from 8 a.m. to 5 p.m., these results assume not all occupants leave real buildings at the same time. This allows for real world factors such as small numbers of professional staff or cleaning staff adjusting blinds at other hours. Additionally, the Blindswitch algorithms assume some amount of hysteresis with a delay in blind retraction. The other four facades typically result in single engagement scenarios, with respect to the general shape of annual occlusion. The East façade typically begins engaging blinds at 6 a.m. and retracts around 4 p.m. because of the movement of the sun. Peak blind engagement occurs at 9:30 a.m. in the month of July.

The South façade has a unique response to occlusion of blinds. As expected, peak blind engagement occurs during winter months as the sun rises later and falls earlier in the day but is lower in the sky.

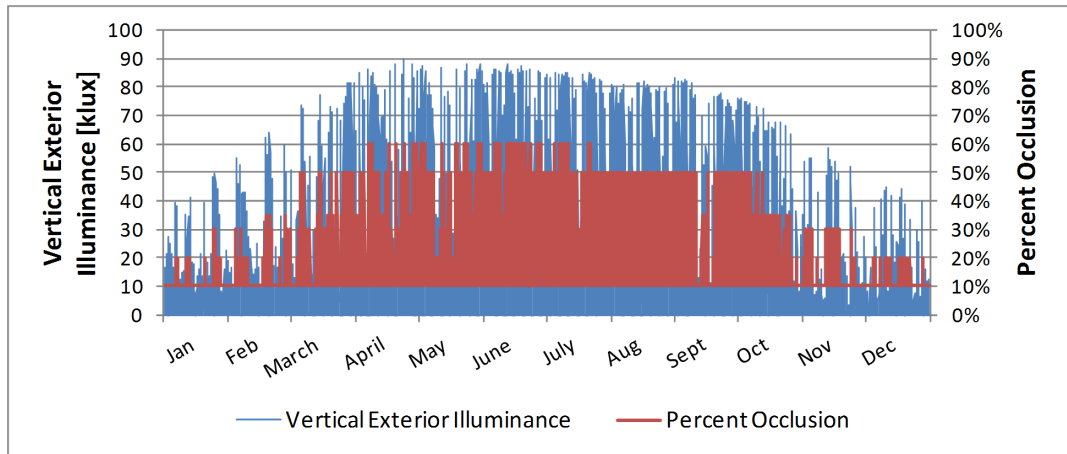
The West façade mimics a mirrored image of east facades response. Blinds begin engaging around 2 p.m. and peak occlusion occurs at 6 p.m. in June. The results follow a similar trend as the days move toward the summer months such that full retraction occurs later in the day. This trend flips as the year progresses, resulting in shorter periods of occlusion, earlier in the day as summer transitions to fall and winter.



**Figure 13.** Hourly average percent occlusion for second floor (Blindswitch A).

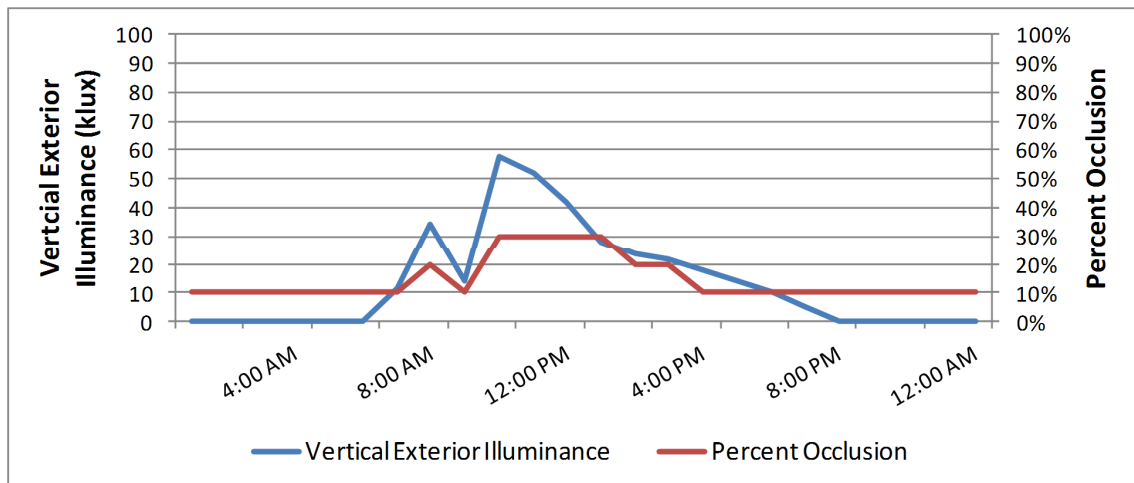
### 3.2.2. Blindswitch-2012B

Figure 14 shows the vertical exterior illuminance *versus* percent occlusion on the East façade of the first floor on an annual basis for Blindswitch B. The winter months result in less blinds engaging while the summer months result in peak occlusions of 60%. Full blind engagement (70%) was never met on this façade because exterior illuminance does not reach the trigger value of 100,000 lux.



**Figure 14.** Annual vertical exterior illuminance vs. percent occlusion for the east facade first floor (Blindswitch B).

Figure 15 shows the response to the control algorithm for a single day on the East façade first floor. This shows the proportional relationship between the two factors; more window blinds engage with increasing vertical illuminance.



**Figure 15.** Control algorithm responses (Blindswitch B) on 22 April.

Blind occlusion values for Blindswitch B followed the same response as Blindswitch A but on a smaller scale. Overall, the South façade resulted in the largest average occlusion percentage, as seen in Figure 16. The North façade results in the minimum occlusion of 10% due to the fixed blinds that are always engaged. For Blindswitch B, the north façade does not engage operable blinds because vertical exterior illuminance never rises above the minimal trigger of 33,000 lux. This effect can also be seen in the color map of Blindswitch B (Figure 17). The Northeast and East facade increase average occlusion with floor height. Conversely, the West façade slightly decreases average occlusion as floor height increases.

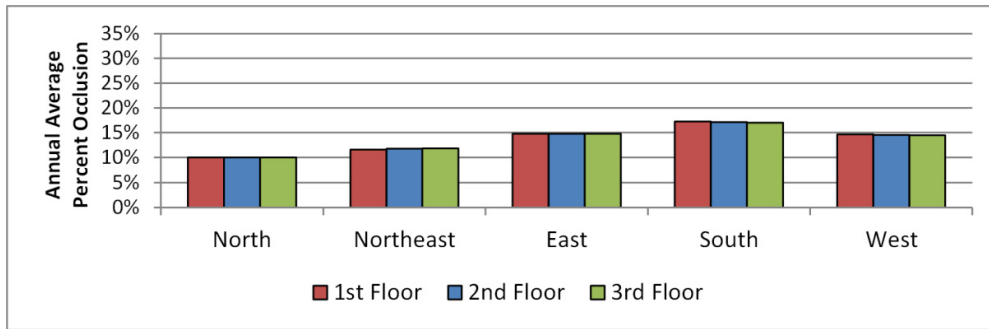


Figure 16. Annual average percent occlusion (Blindswitch B).

Figure 17 displays color maps with average occlusion values as a function of hour of day and month of year for the second floor. On the East façade, blinds begin to engage around 6:30 a.m. and typically retract around 0:30 p.m. The South façade results in blinds engaging around 9:30 a.m. and retracting around 5:30 p.m. There was a lower average percent of occlusion during the middle of the year for the South façade, as seen in Blindswitch A. The West façade also shows a similar response as found in Blindswitch A, and has a peak occlusion for the entire model of around 60% at 5 p.m. in May.

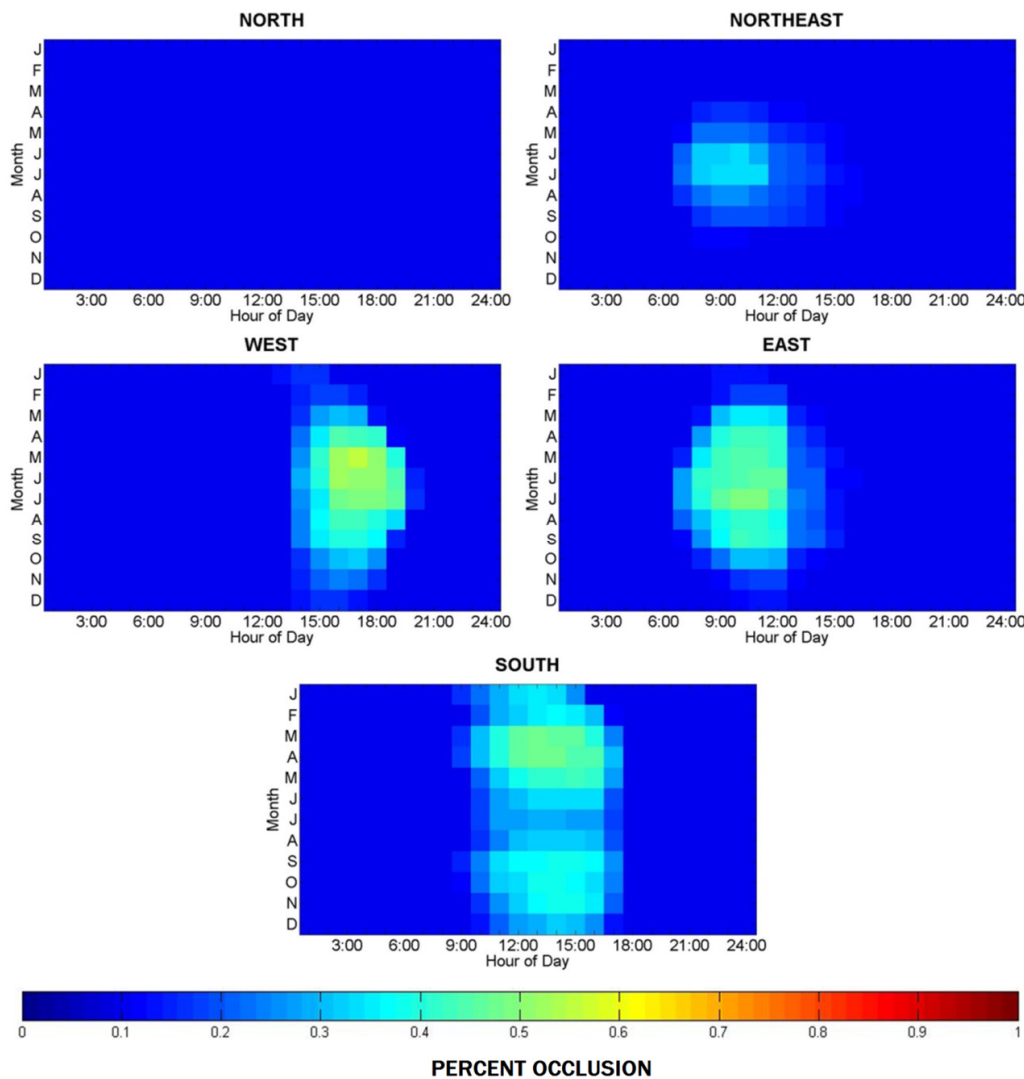


Figure 17. Hourly average percent occlusion for second floor (Blindswitch B).

3.2.3. DGI<sub>20</sub>

Figure 18 shows the annual average percent occlusions for each orientation for the DGI<sub>20</sub> algorithm. In all orientations except for the North façade the 3rd floor resulted in the smallest average occlusion. The South façade on the second floor had the largest peak average occlusion value of 31.5%. Overall, DGI<sub>20</sub> does not show conclusive results of glare response specifically due to orientation and floor height.

One limitation of the glare calculation used by EnergyPlus is that it does not take into account glare caused by beam radiation coming through the window with a retracted blind. Therefore, the DGI<sub>20</sub> algorithm potentially under predicts occlusion due to neglecting glare caused by direct sun. This is due to the simplified glare analysis based on average calculations of luminance of the window seen from a reference point and luminance background area surrounding the window.

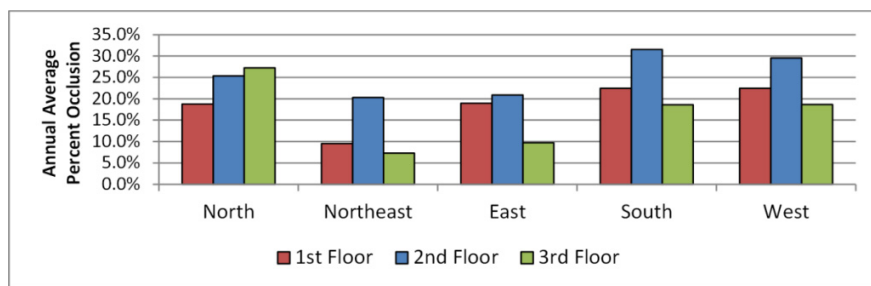


Figure 18. Annual average percent occlusion (DGI<sub>20</sub>).

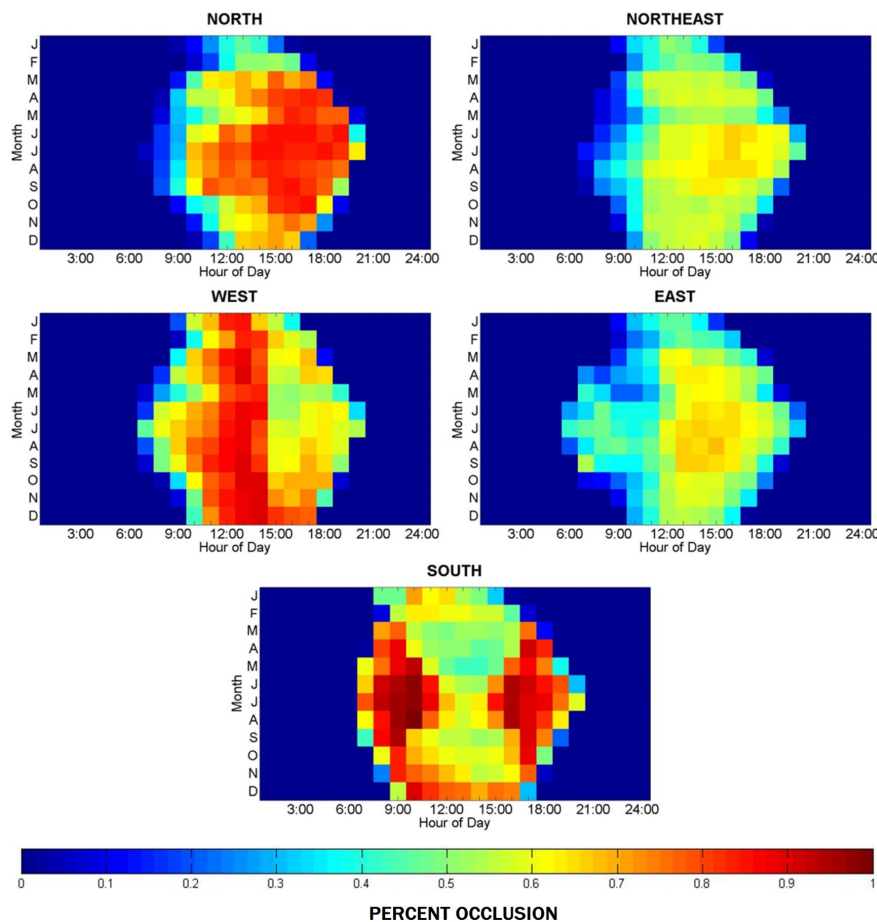
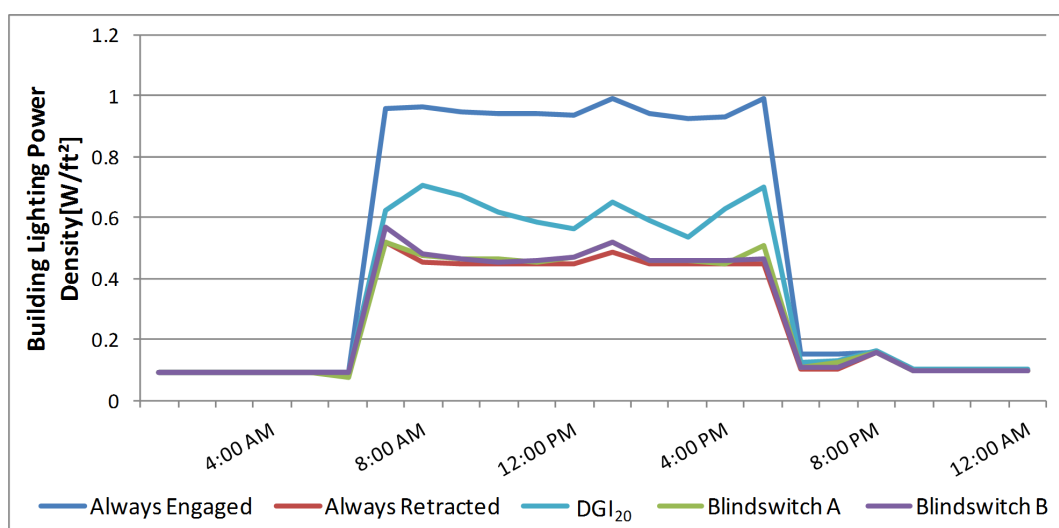


Figure 19. Hourly average percent occlusion for second floor (DGI<sub>20</sub>).

Figure 19 shows the color map representation of hourly average occlusion percentage. The hour of the day is on the x-axis, and the month of year is on the y-axis. Dark red and dark blue correspond to full blind engagement and full retraction, respectively. The Northeast and East façade results show similar average occlusion levels, with a peak occlusion of 67% occurring in May at 3 p.m. The South façade shows full blind engagement (100% since there was no limit as is the case in Blindswitch A and B) at 10 a.m. and 5 p.m. in the summer months. Interestingly, the South façade results show that blinds engaging due to glare increases as summer reaches its peak during July, and subsides as the year continues into the winter months (early and late in the year), much different than was found with the Blindswitch algorithms. The North façade typically results in peak occlusion during the afternoon summer months.

### 3.3. Lighting Loads

Building lighting power density for the five blind control algorithms is compared in Figure 20. While each method employs different metrics for triggering blind occlusion, this comparison provides insight to their relative differences with regard to lighting energy savings from daylight harvesting. The blind control algorithms were compared on 25 July. This day was chosen for comparison because it contains a typical sunny summer day. This day helps demonstrate the variability of the blind control algorithms and the lighting response to each. The actual building utilizes standard T8 fixtures with a building lighting power density of  $1.27 \text{ W/m}^2$ . Each algorithm shows the same basic response of turning on lights at 6 a.m. and turning off around 6 p.m. (due to prescribed occupancy schedules) with variance shown as a result of available daylight due to blind control differences. Once interior lighting levels reach 322 lux, the recommended minimum lighting level for office spaces [20], the electric lighting is completely turned off. Though there are several driving factors of lighting control, for this study lights were given specific schedules which follow the occupancy load. If daylight was available within those occupied hours then electric lights are dimmed. The study aimed to isolate the real effect of blind control, so other confounding factors impacting real world lighting control were held constant.



**Figure 20.** Fractional hourly electric light output comparison on 25 July.

The variability occurred in the middle of the day when the level of fractional increase varies with each control algorithm. The Always Retracted algorithm allows the most amount of daylight, resulting in the lowest lighting energy demand. Other possible blind trigger variables were not considered across the individual algorithms. Of the multiple blind control algorithms included in this study, DGI<sub>20</sub> explicitly addresses a simplified glare analysis, whereas Blindswitch A and B implicitly includes glare along with other human factors. By isolating these variables it provides insight of how each variable responds compared to the others. Conversely, Always Engaged allows the least amount of daylight, resulting in the highest lighting energy demand. As expected, DGI<sub>20</sub> results in a larger lighting demand than Blindswitch A, Blindswitch B, and Always Retracted due to the typically larger percentage of blind occlusion throughout the year. Blindswitch A, Blindswitch B, and Always Retracted algorithms result in similar lighting demand response.

### 3.4. Annual Energy Consumption

Figure 21 compares the EUI for the building by end use. End-uses such as fans, pumps, water systems, and heat rejection had very similar total results regardless of the applied blind control algorithm so they were combined into one category in the figure. Annual consumption was compared for each manual blind algorithm against the baseline model which does not include blinds or daylight harvesting control. The blind control algorithms Always Engaged and Blindswitch A have relative difference in total consumption of 8.1%. This leads to the conclusion that when strictly comparing end-uses, such as with baseline calibration, a sophisticated manual blind control algorithm varies substantially from the static algorithms. The three dynamic blind control algorithms vary, with respect to lighting consumption of the Always Engaged algorithm (baseline model with blinds closed and daylight sensing electric lighting controls added), from 28.9% to 39.4% higher annual energy consumption. Compared to the Always Retracted algorithm lighting consumption varies less significantly with overall lower energy consumption, 3.6%–21.8%. Cooling consumption differences for the sophisticated blind control algorithms range absolutely from 8.6% to 9.0% and 0.8%–3.6% compared to the Always Engaged and Always Retracted algorithms, respectively. Heating consumption differences for the advanced algorithms range absolutely from 6.6% to 27.2% and 0.8%–15.9% compared to the Always Engaged and Always Retracted algorithms, respectively.

Figure 21 also includes results from both internal (IB) to external blinds (EB) for the Blindswitch A and B, DGI<sub>20</sub>, and Always Engaged control algorithms. Energy use intensity reductions are based upon differences from the baseline model, which employs blinds always retracted but without simulated lighting reduction due to incorporation of daylight harvesting. Energy savings seen from direct comparison to internal blind models are caused by external blinds blocking solar heat loads before they ever reach the window. Total energy consumption reductions of 8.1%–18.5%, or 16.2–55.4 kWh/m<sup>2</sup>·year was seen amongst the four models compared to the baseline model. Always Engaged results in the largest energy reduction by switching from interior blinds to exterior blinds, while Blindswitch B with exterior blinds shows the lowest overall energy consumption of all models.

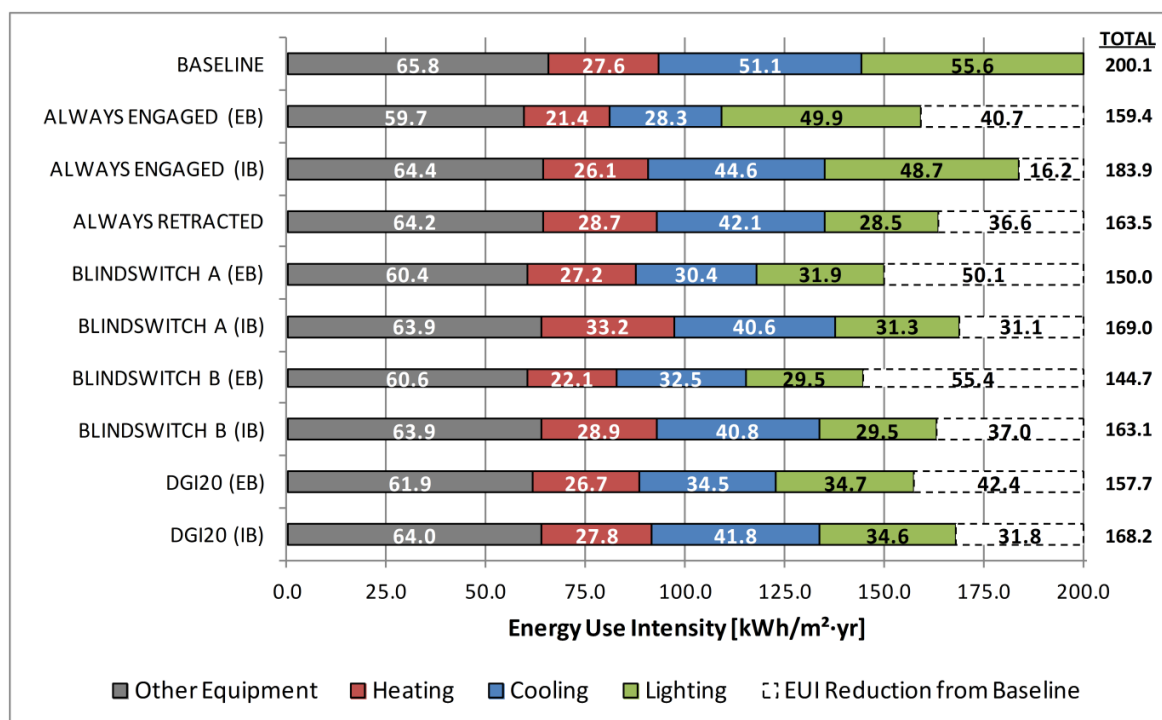


**Figure 21.** Annual end-use energy consumption comparison of interior (IB) and exterior blind (EB) algorithms.

All blind control algorithms result in overall energy savings increases compared with the Always Engaged (IB) algorithm, primarily in the lighting end use. It becomes evident that blind control algorithms should be included in simulation best practices to account for the variability of both solar gain and manual blind operation likely to occur in real buildings. If a blind control algorithm is used, it will create a more realistic model but may consequently require further simulation effort to account for the difference between the model and the actual baseline energy use consumption (*i.e.*, increase heating, cooling, *etc.*) when calibrating models to existing buildings. Calibration results are compared to highlight the energy consumption effect of incorporating manual blind control algorithms. ASHRAE Guideline 14–2002 [13] recommends coefficient of variance of the mean square error (CVRMSE), seen in Equation (7), and normalized mean bias error (NMBE), seen in Equation (8), as two statistical analyses for calibration of monthly whole building simulation:

$$CVRMSE = 100 \cdot \frac{\left[ \frac{\sum (y_i - \hat{y}_i)^2}{(n - p)} \right]^{1/2}}{\bar{y}} \quad (6)$$

$$NMBE = \frac{\sum^n (y_i - \hat{y}_i)}{(n - p) \cdot \bar{y}} \cdot 100 \quad (7)$$

The parameter  $y_i$  is the actual building consumption,  $\hat{y}_i$  is predicted consumption,  $n$  is the number of data points used,  $p$  is the number of terms in the baseline model,  $\bar{y}$  is the mean of the sample.

Table 6 shows the CVRMSE and NMBE values for each blind control algorithm with interior blinds. Guideline 14 does not specify if both statistical indices must be met. NMBE indicates how well the model predicts energy consumption. However, NMBE is subject to cancellation errors brought on by positive and negative values. A positive value corresponds to over prediction of actual data;

negative values relate to under prediction of actual data. To account for this error, CVRMSE is used as well, which indicates the overall uncertainty of energy prediction. A maximum value of  $\pm 15\%$  is acceptable for CVRMSE, and  $\pm 5\%$  is acceptable for NMBE. Blindswitch A and Always Engaged yield consumption data that are the closest to being calibrated to real building consumption, yet all five models are statistically un-calibrated without further model manipulation. The real building calibration was based on using the Always Retracted scheme without including lighting reductions from use of daylight harvesting. By introducing these blind control schemes their respective annual consumption results are different than that of the original model. This means further calibration would need to be performed if such control schemes were accepted.

**Table 6.** Statistical indices for calibration.

Statistical Index	Baseline	Always Engaged	Always Retracted	Blindswitch A	Blindswitch B	DGI <sub>20</sub>	Maximum Allowable
CVRMSE	10.67%	17.66%	19.02%	21.69%	19.30%	23.22%	$\pm 15\%$
NMBE	-4.69%	9.27%	10.89%	18.94%	11.82%	19.30%	$\pm 5\%$

### 3.5. Peak HVAC Loads

Peak loads are used to help identify important aspects of building design including system and zonal component sizing. An exaggerated load can have adverse effects on overall project implementation such as oversized equipment, which results in increased capital costs and in some cases decreased system efficiency due to part load performance. Oversized systems can also cause decreased run cycles, reducing the ability to effectively dehumidify a space. This also reduces the life span expectancy of some types of equipment. Because the case study building was internally load dominated, only the peak loads for perimeter zones are compared. Results show that peak heating and cooling loads on a zonal level, for all five blind control algorithms with internal blinds, show similar responses [14].

The Always Retracted algorithm, with interior blinds, results in the smallest peak cooling load caused by a reduction in lighting load. The Always Engaged algorithm, also with interior blinds, results in the largest peak cooling load compared to the other algorithms; a 7.2%–9.8% peak load increase. This algorithm consequently results in the largest heating load affected by lack of supplemental solar heat gain, compared to the other five control schemes. Results show peak heating differences, from the Always Engaged algorithm, ranging from 4.5% to 5.7% higher compared to the other four manual blind control algorithms. A peak cooling loads comparison draws a slightly larger differential: 7.2%–9.8% higher compared to the Always Engaged algorithm for the other four manual blind control algorithms. Blindswitch A, B, and DGI<sub>20</sub> show similar results for heating and cooling design loads.

## 4. Discussion and Conclusions

The main purpose of this research was to assess the impact of applying alternate sophisticated manual blind control algorithms to a previously calibrated energy model to determine the energy and peak demand implications and possible impact upon calibration and modeling best practices. The thermal analysis program EnergyPlus was used to compare relative differences between five reasonable manual blind control candidates for use in lighting and energy simulation. Blind control

was shown to affect multiple aspects of building performance including: lighting, heating, and cooling energy consumption, even in the internally load dominated case study building. Percentage annual energy consumption differences from the baseline model, depending upon the manual blind control algorithm used, range from 8.1% to 18.3% for internal blinds. This corresponds to EUI differences of 16.2–36.6 kWh/m<sup>2</sup>·year in the case study building. Annual differences compared to the Always Retracted algorithm (baseline model with daylight sensing electric lighting controls) range from 0.2% to 11.1% for internal blinds. This corresponds to EUI differences of 0.3–20.5 kWh/m<sup>2</sup>·year. Therefore, manual blind control must be taken into account when performing calibration of an energy model to existing buildings and when using energy models to evaluate design alternatives and system sizing in new buildings.

The case study building was dominated by core zones, therefore future work should include a building with a higher potential for daylight zones to influence building performance (externally load dominated) in order to better demonstrate the effect manual blind control has on energy consumption for that type of building form. External blinds were compared to internal blinds resulting in more energy reduction due to incorporation of external blinds. This was because the peak cooling loads and solar heat gains are blocked before they ever hit the window. Future work should continue to update the proposed manual blind control algorithms Blindswitch A and Blindswitch B as more human factors behavioral data become available. A useful case study would include simulation using measured blind usage data from a specific real building. This would include blind operation reasoning dependent upon façade orientation to determine the effect of blind operation on calibration of simulation more precisely. This would allow for a direct comparison between real data and simulated manual blind control algorithms for continued refinement of these algorithms and recommendations for adoption of a specific algorithm in simulation best practices.

Average hourly occlusion, daily rate of change, and number of blind movement results show that DGI<sub>20</sub> results in unrealistically active manual blind control patterns compared to literature available [5]. A higher blind rate of change typically results in a larger number of blind movements. Because glare is dependent on occupant view and position, analysis points on the North façade actually see a west-facing angle of sight (20° towards a north facing window corresponds to an absolute angle of 290°). The effect of this relationship between view angle and façade orientation are displayed in the average hourly occlusion graph where the North façade shows an unusually large percentage of occlusion. The East and Northeast facades show lower occlusion values because the analysis points are facing the North direction.

Two equations were introduced to solidify the calculation of blind rate of change (ROC) and the number of blind movements (NBM). Results show that Blindswitch A has a whole building average ROC of 38.4% which was similar to results found in the literature (37%) [19]. Blindswitch B whole building average daily ROC of 17.2% matches results found by Sze (17%) [21]. The DGI<sub>20</sub> algorithm results in the largest building average ROC of 60.5% which shows that the model grossly exaggerates blind movement compared to available literature. DGI<sub>20</sub> also resulted in the largest building average NBM of 2.6, followed by Blindswitch A with 1.74, and Blindswitch B with 1.1. Use of DGI<sub>20</sub> is therefore cautioned in simulation best practices due to possible overly active blind use patterns.

For three of the blind control algorithms (Blindswitch A, Blindswitch B, and DGI<sub>20</sub>) blind position continued to change past typical operation hours. This represents an unrealistic scenario, given that an

occupant would most likely leave a blind in the same position at the end of the day. Future enhancements to each algorithm should incorporate more realistic occupancy patterns which will affect blind use because manual blinds cannot be adjusted without the presence of an occupant. The literature suggests that ASHRAE recommended occupancy diversity factors are exaggerated [22]. This would indicate more accurate occupancy patterns will generally lower (perhaps modestly) rate of change. All algorithms were simulated without exterior obstructions such as trees and adjacent buildings. Future research should include these obstructions which would likely modify results by floor in some cases.

Statistical analysis using CVRMSE and NMBE show that applying Blindswitch A results in the smallest numerical uncertainty in comparison with actual energy consumption data, followed closely by the Always Engaged algorithm. Although ASHRAE Guideline 14–2002 does not require both CVRMSE and NMBE, ideally both should be used to achieve a more accurate model. Is it worth the effort of applying a sophisticated manual control algorithm as opposed to a much simpler algorithm such as one of the two extreme conditions (Always Engaged or Always Retracted) to simulate real blind usage? The recommendations of the authors are as follows: (1) Manual blind control schemes should be included to generate accurate lighting and energy performance and Blindswitch A and Blindswitch B appear to follow current field study data more closely than the other algorithms tested; (2) applying the Always Engaged algorithm creates a reasonable representation of overall annual consumption for the building studied, but fails to mimic accurate lighting and heating demand due to the interaction between the two (practically speaking, it would be valuable to conduct simulations with blinds Always Retracted and Always Engaged to understand the range of sensitivity to blind use patterns in buildings and subsequent range of energy use and peak demand associated with alternate design decisions); and (3) further field studies are needed to better understand blind usage with respect to building type, location, climate, view quality, and orientation. This would allow for more accurate generalizations and help understand specific reasoning for manual blind usage. Furthermore, given that most of the literature suggests that blinds are controlled dominantly to ensure visual comfort, as metrics are introduced regarding visual comfort and glare in settings with daylight, updates to Blindswitch-2012A and Blindswitch-2012B may be warranted.

### **Acknowledgments**

We would like to thank the Integrated Design Lab, affiliated with the University of Idaho, for creating a positive and sustainable research environment for engineering students.

### **Author Contributions**

Christopher Dyke was the main author for this paper as a continuation of his thesis work for Masters of Science in Mechanical Engineering at the University of Idaho. Kevin Van Den Wymelenberg (Professor of Architecture at the University of Idaho), Ery Djunaedy (Building Simulation Scientist at the University of Idaho), and Judi Steciak (Professor of Mechanical Engineering at the University of Idaho) served as co-authors providing technical support and guidance throughout the research period.

## Conflicts of Interest

The authors declare no conflict of interest.

## References

1. Bourgeois, D.; Reinhart, C.; Macdonald, I. Adding advanced behavioral models in whole building energy simulation: A case study on the total energy impact of manual and automated lighting control. *Energy Build.* **2006**, *38*, 814–823.
2. Correia da Silva, P.; Leal, V.; Andersen, M. Influence of shading control patterns on the energy assessment of office spaces. *Energy Build.* **2012**, *50*, 35–48.
3. Newsham, G. Manual control of window blinds and electric lighting: Implications for comfort and energy consumption. *Indoor Environ.* **1994**, *3*, 135–144.
4. Reinhart, C. Lightswitch-2002: A model for manual and automated control of electric lighting and blinds. *Sol. Energy* **2004**, *77*, 15–28.
5. Van Den Wymelenberg, K. Patterns of occupant interaction with window blinds: A literature review. *Energy Build.* **2012**, *51*, 165–176.
6. Zhang, R.; Lam, K.P. Comparison of building load performance between first principle based and implementable shading control algorithms. *Build. Simul.* **2011**, *4*, 135–148.
7. Palmero-Marrero, A.; Oliveira, A.C. Effect of louver shading devices on building energy requirements. *Appl. Energy* **2010**, *87*, 2040–2049.
8. Bader, S. High Performance Facades for Commercial Buildings. Master Thesis, University of Texas at Austin, Austin, TX, USA, May 2010.
9. Reinhart, C.; Mardaljevic, J.; Rogers, Z. Dynamic daylight performance metrics for sustainable building design. *Leukos* **2006**, *3*, 1–25.
10. Congradac, V.; Prica, M.; Paspalj, M.; Bojanic, D.; Capko, D. Algorithm for blinds control based on the optimization of blind tilt angle using a genetic algorithm and fuzzy logic. *Sol. Energy* **2012**, *86*, 2762–2770.
11. Lee, E.S.; Fernandes, L.L.; Coffey, B.; McNeil, A.; Clear, R.D.; Webster, T.L.; Bauman, F.S.; Dickerhoff, D.J.; Heinzerling, D.; Hoyt, T. *A Post-Occupancy Monitored Evaluation of the Dimmable Lighting, Automated Shading, and Underfloor Air Distribution System in the New York Times Building*; LBNL-6023E; Lawrence Berkeley National Laboratory: Berkeley, CA, USA, 2013.
12. Chauvel, P.; Collins, J.B.; Dogniaux, R.; Longmore, J. Glare from windows: Current views of the problem. *Light. Res. Technol.* **1982**, *14*, 31–46.
13. *Measurement of Energy and Demand Savings*; ASHRAE Guideline 14-2002; American Society of Heating, Refrigeration and Air-Conditioning Engineers, Inc. (ASHRAE): Atlanta, GA, USA, 2002.
14. Dyke, C. A Comparison of Manual Blind Control Algorithms Using Two Methods of Daylight Harvesting Simulation. Master Thesis, University of Idaho, Moscow, ID, USA, May 2013.
15. Saxena, M.; Ward, G.; Perry, T.; Heschong, L.; Higa, R. Dynamic Radiance—Predicting Annual Daylighting with Variable Fenestration Optics Using BSDFs. In Proceedings of the Fourth National Conference of IBPSA-USA, New York, NY, USA, 11–13 August 2010.

16. Foster, M.; Oreszczyn, T. Occupant control of passive systems: The use of venetian blinds. *Build. Environ.* **2001**, *36*, 149–155.
17. Winkelmann, F.; Selkowitz, S. Daylighting simulation in the DOE-2 building energy analysis program. *Energy Build.* **1985**, *8*, 271–286.
18. Inoue, T.; Kawase, T.; Ibamoto, T.; Takakus, S.; Matsuo, Y. The development of an optimal control system for window shading devices based on investigations in office buildings. *ASHRAE Trans.* **1988**, *104*, 1034–1049.
19. Lindsay, C.R.T.; Littlefair, P.J. *Occupant Use of Venetian Blinds in Offices*; 233/92; Building Research Establishment: Watford, UK, 1992.
20. *Code of Federal Regulations (CFR) Title 29—Labor*; U.S. Department of Labor: Washington, DC, USA, 2009.
21. Sze, J.L. *Indoor Environmental Conditions in New York City Public School Classrooms Survey*; Harvard University: Cambridge, MA, USA, 2009.
22. Duarte, C. Revealing Occupancy Patterns in Office Buildings through the Use of Sensor Data Providing Whole Building Energy Simulation. Master Thesis, University of Idaho, Moscow, ID, USA, May 2013.

© 2015 by the authors; licensee MDPI, Basel, Switzerland. This article is an open access article distributed under the terms and conditions of the Creative Commons Attribution license (<http://creativecommons.org/licenses/by/4.0/>).